Transitions Between the $^2\Pi_{1/2}$ and $^2\Pi_{3/2}$ Spin-Orbit Components of NO Induced by Impact of Slow Electrons

Michael Allan
Department of Chemistry, University of Fribourg, Switzerland
(Dated: June 4, 2004)

Electron impact cross section for the transition between the $^2\Pi_{1/2}$ and $^2\Pi_{3/2}$ spin-orbit components of the ground electronic term of nitric oxide, separated by 15 meV, has been measured as a function of electron energy at a scattering angle of $\theta = 135°$. It is dominated by the $^3\Sigma^-$ and the $^1\Delta$ resonances. Its magnitude is very large, at peak about equal to that of the elastic cross section. The elastic cross sections for the two components have also been determined.

PACS numbers: 34.80.Gs

Introduction.—The knowledge of the interactions of slow electrons with nitric oxide is important because NO is used as a plasma gas. Moreover, it has an unpaired electron and thus offers an opportunity to study electron collisions with radicals. Radicals are often formed by electron-impact dissociation of molecules in plasmas and are important plasma species. Little is known about their interaction with free electrons, however, because they are generally chemically very reactive and difficult to feed into electron spectrometers. Nitric oxide is thus an important prototype case, permitting the study of the basic principles in collisions of electrons with radicals.

An important consequence of the unpaired electron, absent in molecules with closed electron shell, is that electronic terms with nonzero orbital angular momentum are split into spin-orbit components. The $^2\Pi$ ground electronic term of NO is split into two components ('substates'), $^2\Pi_{1/2}$ and $^2\Pi_{3/2}$ [1]. Their interactions with free electrons have not been studied individually because they are separated by only $\Delta E_0 = 15$ meV and are hard to resolve. This work makes use of the recent instrumental progress [2] in terms of resolution and low energy capacity to investigate into what degree can collisions with slow electrons induce transitions between the two spin-orbit components. The present work is oriented primarily towards the properties of NO relevant in plasmas, but it is worthwhile noting that nitric oxide has recently received much publicity because of the unexpected and multifaceted role which it plays in biology [3].

There are numerous electron collision studies on NO which do not distinguish the two spin-orbit components. They revealed sharp structures due to the $^3\Sigma^-$ and the $^1\Delta$ resonances of NO^- [4–8]. Interpretation of these structures yielded the NO^- internuclear separation $r_e(NO^-) = 1.262(+0.005, -0.025)$ Å [9]. Precise quantitative elastic and vibrational excitation cross sections have been measured more recently [10, 11]. The resonances were also studied on NO cooled by supersonic expansion [12]. Resonance parameters for the low-lying states of NO^- were calculated using the R-matrix method [13]. A transition between the spin-orbit components requires that either spin or orbital angular momentum is exchanged between the free electron and the target. The present work is thus related to the spin exchange studies using polarized electrons [14, 15]. Photodetachment studies [16, 17] determined the electron affinity, the latter study yielding the value of 0.026 ± 0.005 eV, together with an independent value for the NO^- internuclear separation $r_e(NO^-) = 1.271 \pm 0.005$ Å.

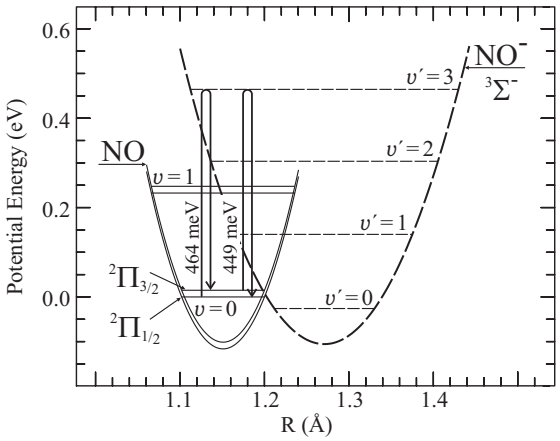

FIG. 1: Schematic potential curves of NO (solid) and NO^- (dashed). The arrows indicate the resonant inelastic and superelastic transitions which can be seen in the spectra of Fig. 2.

Experiment.—The measurements were performed using a spectrometer with hemispherical analyzers [2, 18]. The energy resolution was about 10 meV in the energy-loss mode, corresponding to about 7 meV in the incident electron beam, at a beam current of around 40 pA. The energy of the incident beam was calibrated on the 19.365 eV [19] ^{2}S resonance in helium and is accurate to within ±10 meV. The analyzer response function was determined on the elastic scattering in helium. NO was introduced through a 0.25 mm effusive nozzle kept at ∼30°C. The backing pressure was about 1.1 mbars (around 0.1 mbars when measuring the absolute value). Absolute values of the cross sections were determined by comparison with the theoretical helium elastic cross section [20], using the relative flow method, and are accu-

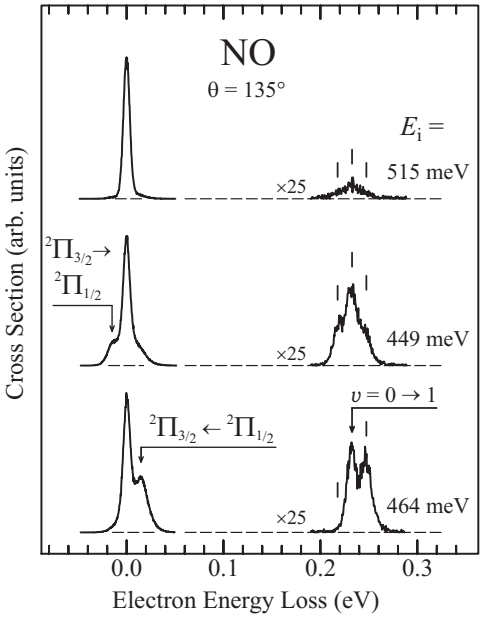

FIG. 2: Electron energy loss spectra of NO.

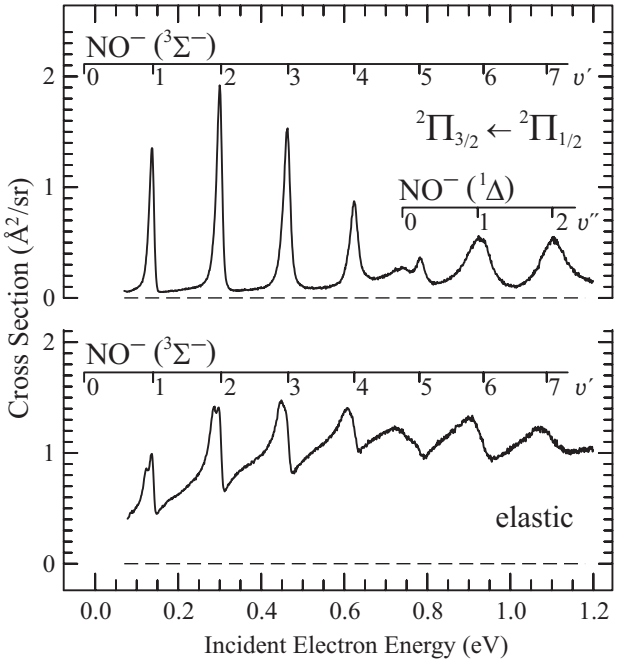

FIG. 3: The elastic (bottom) and the $^2\Pi_{3/2} \leftarrow {}^2\Pi_{1/2}$ inelastic (top) cross sections, measured at $\theta = 135^\circ$. The elastic cross section is shown as measured for the room temperature sample. It is thus a superposition of the elastic cross sections for NO in the $^2\Pi_{1/2}$ and in the $^2\Pi_{3/2}$ states, weighted in the proportion of their thermal populations. The vibrational levels of the $^3\Sigma^-$ and the $^1\Delta$ states of NO^- are indicated.

rate within ±25%. The measurements were carried out at a representative scatering angle, $\theta = 135^\circ$, which was chosen large to diminish possible contributions of direct excitation. Preliminary measurements at 30°, 90°, and 180° indicate, however, that the shapes of the curves depend little on scattering angle.

Results and Discussion.—Fig. 1 shows the relevant potential curves and vibrational levels of NO and NO^-, based on the known spectroscopical constants [21]. The NO^- vibrational levels higher than $v' = 0$ are resonances, subject to autodetachment of an electron.

Fig. 2 shows electron energy loss spectra recorded at constant incident electron energies. The incident energy in the bottom spectrum, $E_i = 464$ meV, was chosen such as to excite the $^3\Sigma^-(v' = 3)$ resonance. The peak corresponding to the *inelastic* $^2\Pi_{3/2} \leftarrow {}^2\Pi_{1/2}$ transition is prominent at this incident energy. The incident energy in the center spectrum, 449 meV, was chosen such as to excite the same $^3\Sigma^-(v' = 3)$ resonance starting from the thermally populated $^2\Pi_{3/2}$ substate of NO. This time it is the peak corresponding to the $^2\Pi_{3/2} \rightarrow {}^2\Pi_{1/2}$ *superelastic* transition which is prominent. Both the inelastic and the superelastic peaks are weak in the top spectrum, where no resonance can be reached. Similar peaks, but this time accompanied by the excitation of one vibrational quantum of NO, are seen on the right side of Fig. 2. These transitions will not be studied in detail here.

Note that about 64% of the NO molecules in the target gas are in the $^2\Pi_{1/2}$ substate and 36% are in the $^2\Pi_{3/2}$ substate (see below). The elastic peaks in Fig. 2 are due to all target NO molecules, the inelastic peak only to those originally in the $^2\Pi_{1/2}$ substate. It is thus evident already at this level that the cross section for the electronically inelastic transition must be very large, similar to the elastic cross section. The same must be true when vibration is co-excited: Both the electronically elastic and the electronically inelastic peaks on the right side of the bottom spectrum in Fig. 2 are of comparable height.

The top trace of Fig. 3 shows the electronically inelastic cross section as a function of the incident electron energy. It is dominated by the resonant excitation, the signal between the resonant peaks is only weak. (Part of the weak signal between the peaks could actually be due to elastic scattering since the elastic and the inelastic peaks partially overlap – see Fig. 2).

The absolute value of the inelastic cross section was determined by measuring the apparent absolute value using the relative flow method, where the total density of NO is taken as a base, and dividing it by 0.64, the fraction of NO in the $^2\Pi_{1/2}$ component. The ratio of the thermal populations of the two components was obtained [1] as

$$\frac{n_{3/2}}{n_{1/2}} = \frac{\sum_{J=3/2}^{\infty}(2J+1)\exp\left[-\beta\left(\Delta E_0 + F_\Omega\left(J\right)\right)\right]}{\sum_{J=1/2}^{\infty}(2J+1)\exp\left[-\beta F_\Omega(J)\right]},$$

where $\beta = 1/(kT)$, the subscripts $\frac{1}{2}$ and $\frac{3}{2}$ denote the electronic (spin and orbit) angular momentum Ω, the energies of the individual rotational levels are $F_\Omega(J) = B\left[J\left(J+1\right) - \Omega^2\right]$ with the total (electronic and rotational) angular momentum $J = \Omega, \Omega+1, \cdots$.

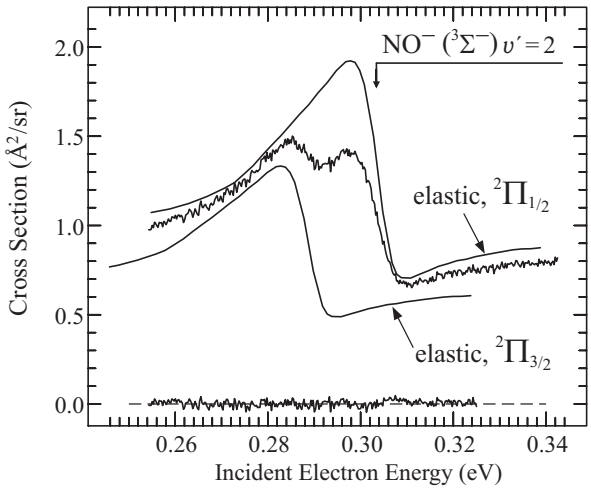

FIG. 4: Elastic cross sections at $\theta = 135°$. The line with statistical noise is the cross section as recorded, averaged over the thermal populations of the two spin-orbit components. The smooth solid lines are the individual elastic cross sections, obtained by deconvolution of the experimental signal and dividing by the thermal populations, as described in text. The residuals, (differences between data and deconvoluted curves) are shown at the bottom. The origin of the $v' = 2$ level of the NO^- $^3\Sigma^-$ resonance is indicated by an arrow.

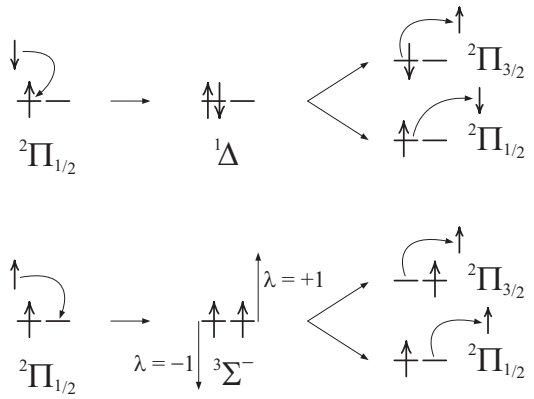

FIG. 5: Electron configurations in the scattering processes *via* the $^3\Sigma^-$ (bottom) and the $^1\Delta$ (top) resonances.

The elastic cross section in Fig. 3, recorded on the thermal mixture of NO in the $^2\Pi_{1/2}$ and $^2\Pi_{3/2}$ substates, has double maxima at the resonant peaks at $v' = 1$ and 2, which are no longer resolved at $v' = 3$ because the width of the resonance increases with v'. The double peak at $v' = 2$ is shown in detail in Fig. 4. It is due to the fact that the sharp resonant feature is reached at a lower incident energy in collisions with NO in the upper substate $^2\Pi_{3/2}$ (see Fig. 1). The double peak can be used to determine the individual elastic cross sections. The measured cross section is first deconvoluted into two curves, with identical shape, separated by 15 meV. The assumption of identical shapes is justified by the excellent agreement of the fit with the experimental curve (indicated by the small residuals in Fig. 4). The two curves resulting from the deconvolution are then divided by the relative populations of the $^2\Pi_{1/2}$ and $^2\Pi_{3/2}$ substates to yield the two elastic cross sections. Surprisingly, the absolute magnitudes obtained in this way are not equal. It is difficult to envisage an experimental error in the determination, however. The accuracy of the deconvolution is better than 5%, leaving only an error in the determination of the relative populations. One would have to assume a target gas temperature of about 190 K to explain the observed spectrum under the assumption of identical magnitudes of the two elastic cross sections. Such cooling does not appear possible with the low backing pressure (1.1 mbars) used here. Furthermore, the shape of the spectrum remained the same with a lower backing pressure of 0.4 mbars.

Note that the elastic and electronically inelastic cross sections of NO in the $^2\Pi_{1/2}$ substate have nearly the same peak magnitudes, about 1.9 $Å^2$/sr (Figs. 3 and 4). This is understandable regarding the electron configurations in the lower part of Fig. 5. Both the $^2\Pi_{1/2}$ and the $^2\Pi_{3/2}$ states are parent states of the $^3\Sigma^-$ resonance. The resonance has consequently two decay channels, with either the electron with its spin parallel, or antiparallel, to its orbital angular momentum λ being ejected, leading to the $^2\Pi_{1/2}$ or $^2\Pi_{3/2}$ states, respectively. Both channels have about the same probability. There is a close analogy between the present transitions as shown in Fig. 5 and the excitation of the low-lying states of O_2, as discussed by Teillet-Billy *at al.* [22].

Both resonant processes should result in spin exchange (the bottom part of Fig. 5 oversimplifies the situation, in reality a $^3\Sigma^-$ scattering complex with $M_s = 0$ will also occur, giving rise to spin exchange). Nearly no depolarisation was observed in experiments with spin-polarized electrons [15] at 2.5 eV, probably because 2.5 eV is too high for the $^3\Sigma^-$ and $^1\Delta$ resonances to have an appreciable effect.

The peaks in the inelastic cross section in Fig. 3 are asymmetrical, and the $v' = 2$ peak, recorded with a slightly higher resolution, is shown in more detail in Fig. 6. The envelope of the $\Delta N = 0$ transitions indicates that the asymmetry is primarily caused by unresolved rotational structure. The rotational width is relatively large, about 9 meV for the $\Delta N = 0$ transitions shown, because the internuclear separations r_e (Fig. 1) and consequently the rotational constants B_e of NO and NO^- are quite different [21]. In reality transitions with $\Delta N = \pm 1$ and ± 2 probably also contribute and make the rotational profile even wider. The width of the experimental band at half height (fwhm) in Fig. 6 is 13.5 meV. Subtracting (taking the root of the difference of the squares) the contributions of the estimated instrumental (7 meV) and $\Delta N = 0$ rotational (9 meV) widths leads to an estimate of the upper limit of the natural width of the

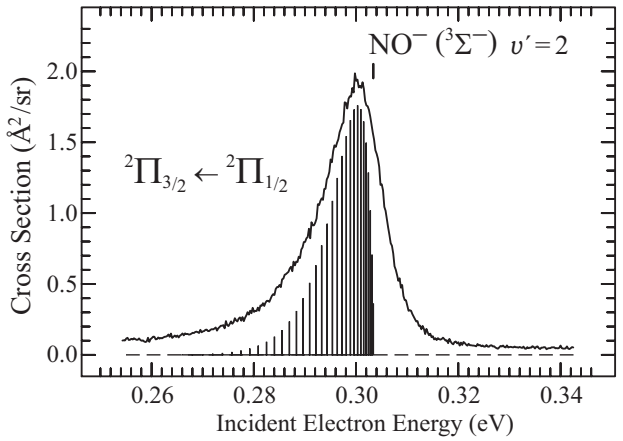

FIG. 6: Detail of the $^2\Pi_{3/2} \leftarrow {}^2\Pi_{1/2}$ inelastic cross section around the $v' = 2$ level of the NO^- $^3\Sigma^-$ resonance. The expected energies of the $\Delta N = 0$ rotational transitions (NO $^2\Pi_{1/2}$ $v = 0 \rightarrow NO^-$ $^3\Sigma^-$ $v' = 2$) are indicated.

NO^- $^3\Sigma^-$ $v' = 2$ resonance to be about 7 meV. This is narrower than reported previously, the narrowest width reported for the $v' = 2$ level was 29 meV [12]. Note that the cross section measured in reference [12] was a superposition of the elastic and electronically inelastic cross sections because the final states were not resolved. On the other hand their spectrum was not rotationally broadened because of supersonic expansion cooling.

The parameters of the NO^- $^3\Sigma^-$ resonance obtained in this work are: Electron affinity 26.8 meV, vibrational constant $\tilde{\nu}_e = 1360$ cm^{-1}, anharmonicity $\tilde{\nu}_e x_e = 9.5$ cm^{-1}. The value of the electron affinity is in a fortuitously good agreement with the (rotationally adjusted) photoelectron value of 0.026 ± 0.005 eV [17]. Note that the present energies are taken slightly to the right of the peak positions as suggested by the rotational profile in Fig. 6, that is, they are also rotationally adjusted. The resonance energies are in good agreement with earlier measurements [7, 12].

The parameters of the NO^- $^1\Delta$ resonance are: Energy of the center of the lowest vibrational level $T_0 = 0.74$ eV, vibrational constant $\tilde{\nu}_e = 1480$ cm^{-1}, anharmonicity $\tilde{\nu}_e x_e = 8$ cm^{-1}. The width of the $v'' = 1$ peak is 80 meV.

Finally it must be pointed out that a detailed description of the electronic fine structure transitions discussed here must take into account that they are interwoven with molecular rotation because of similar energy spacings. The distinction between the $^2\Pi_{1/2}$ and $^2\Pi_{3/2}$ becomes only approximate for higher values of J because of spin uncoupling and transition to Hund's case (b) [1].

Conclusions.—The differential cross section for the $^2\Pi_{3/2} \leftarrow {}^2\Pi_{1/2}$ transition between the spin-orbit components of the ground electronic term of NO was found to have extraordinarily large values at the energies of the NO^- $^3\Sigma^-$ and $^1\Delta$ resonances. The magnitudes are comparable to the values of the elastic cross sections. This is very unusual for an electronic transition. It is because the excitation is mediated by shape resonances, and both attachment and decay of the resonance are one electron processes. This is generally not the case for electronic excitation, because the shape resonance usually lies energetically below the electronically excited state and excitation occurs *via* a core excited resonance, the formation of which involves a two-electron process. The resonance energies are in good agreement with previous work, but the widths are narrower. The present experiment indicates, somewhat surprisingly, that at $\theta = 135°$ the differential elastic cross section of NO in the $^2\Pi_{1/2}$ substate is larger than that of NO in the $^2\Pi_{3/2}$ substate.

I thank G. F. Hanne, H. Hotop and D. Teillet-Billy for valuable comments. This research is part of project No. 2000-067877.02 of the Swiss National Science Foundation.

[1] G. Herzberg, vol. I. Spectra of Diatomic Molecules (Van Nostrand Reinhold Company, N. Y., 1950).
[2] M. Allan, Phys. Rev. Lett. **87**, 033201 (2001).
[3] F. Murad, Bioscience Reports **19**, 133 (1999).
[4] M. J. W. Boness and J. B. Hasted, Phys. Lett. **21**, 526 (1966).
[5] H. Ehrhardt and K. Willmann, Z. Physik **204**, 462 (1967).
[6] D. Spence and G. J. Schulz, Phys. Rev. A **3**, 1968 (1970).
[7] P. D. Burrow, Chem. Phys. Lett. **26**, 265 (1974).
[8] M. Tronc, A. Huetz, M. Landau, F. Pichou, and J. Reinhardt, J. Phys. B **8**, 1160 (1975).
[9] D. Teillet-Billy and F. Fiquet-Fayard, J. Phys. B **10**, L111 (1977).
[10] B. Mojarrabi, R. J. Gulley, A. G. Middleton, D. C. Cartwright, P. J. O. Teubner, S. J. Buckman, and M. J. Brunger, J. Phys. B **28**, 487 (1995).
[11] M. Jelisavcić, R. Panajotović, and S. J. Buckman, Phys. Rev. Lett. **90**, 203201 (2003).
[12] J. Randell, S. L. Lunt, G. Mrotzek, D. Field, and J. P. Ziesel, Chem. Phys. Lett. **252**, 253 (1996).
[13] J. Tennyson and C. J. Noble, J. Phys. B **19**, 4025 (1986).
[14] T. Hegemann, M. Oberste-Vorth, R. Vogts, and G. F. Hanne, Phys. Rev. Lett. **66**, 2968 (1991).
[15] T. Hegemann, S. Schroll, and G. F. Hanne, J. Phys. B **26**, 4607 (1993).
[16] M. W. Siegel, R. J. Celotta, J. L. Hall, J. Levine, and R. A. Bennett, Phys. Rev. A **6**, 607 (1972).
[17] M. J. Travers, D. C. Cowles, and G. B. Ellison, Chem. Phys. Lett. **164**, 449 (1989).
[18] M. Allan, J. Phys. B **28**, 5163 (1995).
[19] A. Gopalan, J. Bömmels, S. Götte, A. Landwehr, K. Franz, M. W. Ruf, H. Hotop, and K. Bartschat, Eur. Phys. J. D **22**, 17 (2003).
[20] R. K. Nesbet, Phys. Rev. A **20**, 58 (1979).
[21] K. P. Huber and G. Herzberg, vol. IV. Constants of Diatomic Molecules (Van Nostrand Reinhold Company, N. Y., 1979).
[22] D. Teillet-Billy, L. Malegat, and J. P. Gauyacq, J. Phys. B **20**, 3201 (1987).